RSC Advances

PAPER

Cite this: *RSC Adv.*, 2019, **9**, 27743

Low-temperature selective catalytic dehydrogenation of methylcyclohexane by surface protonics†

Kent Takise,[a] Ayaka Sato,[a] Shuhei Ogo,[a] Jeong Gil Seo,[ab] Ken-ichi Imagawa,[c] Shigeru Kado[c] and Yasushi Sekine*[a]

Received 4th August 2019
Accepted 26th August 2019

DOI: 10.1039/c9ra06042a

rsc.li/rsc-advances

The methylcyclohexane (MCH)–toluene cycle is a promising liquid organic hydride system as a hydrogen carrier. Generally, MCH dehydrogenation has been conducted over Pt-supported catalysts, for which it requires temperatures higher than 623 K because of its endothermic nature. For this study, an electric field was applied to Pt/TiO_2 catalyst to promote MCH dehydrogenation at low temperatures. Selective dehydrogenation was achieved with the electric field application exceeding thermodynamic equilibrium, even at 423 K. With the electric field, "inverse" kinetic isotope effect (KIE) was observed by accelerated proton collision with MCH on the Pt/TiO_2 catalyst. Moreover, Pt/TiO_2 catalyst showed no methane by-production and less coke formation during MCH dehydrogenation. DRIFTS and XPS measurements revealed that electron donation from TiO_2 to Pt weakened the interaction between catalyst surface and π-coordination of toluene. Results show that the electric field facilitated MCH dehydrogenation without methane and coke by-production over Pt/TiO_2 catalyst.

Introduction

Wide distribution of high-purity hydrogen is anticipated to make it available as a clean secondary energy source: many primary energy resources can be hydrogen sources; and water is the only product of hydrogen combustion. Through the years, various hydrogen distribution systems such as compressed hydrogen, hydrogen liquefaction, and chemical storage using liquid compounds including ammonia and organic hydrides (cycloalkanes) have been examined. Nevertheless, compressed hydrogen requires large-scale systems and high-pressure storage tanks.[1] Liquefied hydrogen is unsuitable for long-term storage because of its attendant evaporation loss (boil-off).[2,3] Although ammonia has been anticipated as a promising hydrogen carrier with a high hydrogen capacity (17.6 wt%), it has high toxicity.[4,5] Organic hydrides are more practical media for long-term storage and for mass transportation in terms of cost effectiveness and safety.[6–8]

Using organic hydrides requires reversible hydrogenation and dehydrogenation reactions proceeding between aromatic and naphthene compounds (*i.e.* cycloalkanes).[6,7] At hydrogen generation sites, aromatics are converted to naphthene compounds by catalytic hydrogenation. The reverse reaction: dehydrogenation of naphthene to aromatics, is conducted at hydrogen consumption sites. Among various liquid organic hydrides, the most well-known and promising system is a methylcyclohexane (MCH)–toluene cycle (hydrogen capacity: 6.1 wt%) by virtue of its nontoxicity and wider range of liquid phase at 178–374 K.[6,7]

Dehydrogenation of MCH is an endothermic reaction (as shown in eqn (1)): an energy-consuming process. This reaction has been performed over a Pt-supported catalyst.[8] Results show high activity for dehydrogenation above 623 K of reaction temperatures.[6,9–11] However, Pt-based catalysts are easily deactivated with coke formation and/or toluene fouling during the reaction.[12–15] Recently, Ir/USY,[16] partially reduced Mo/SiO_2,[17] Pt–Mo/SiO_2 (ref. 11 and 18) catalysts have been reported as effective catalysts for dehydrogenation of MCH.

$$C_7H_{14} \rightarrow C_7H_8 + 3H_2,\ \Delta H^0_{298} = 205\ \text{kJ mol}^{-1} \quad (1)$$

$$C_7H_8 + H_2 \rightarrow C_6H_6 + CH_4,\ \Delta H^0_{298} = -42\ \text{kJ mol}^{-1} \quad (2)$$

Feasibility of the organic hydride system depends on the product selectivity and lifetime of MCH dehydrogenation catalysts. A side-reaction of MCH dehydrogenation, hydrodemethylation of toluene (as shown in eqn (2)), and coking on the catalyst are key difficulties to be overcome.[19–22] They lead to production of benzene and methane as by-products, thereby

[a]*Waseda University, Department of Applied Chemistry, 3-4-1, Okubo, Shinjuku, Tokyo, 169-8555 Japan. E-mail: ysekine@waseda.jp*

[b]*Myongji University, Department of Energy Science and Technology, 116 Myongji-ro, Yongin-si, Gyeonggi-do 17058, Republic of Korea*

[c]*R&D Center, Chiyoda Corporation, 3-13, Moriya-cho, Yokohama, Kanagawa, 221-0022, Japan*

† Electronic supplementary information (ESI) available. See DOI: 10.1039/c9ra06042a

increasing the costs of hydrogen purification.[19] Furthermore, benzene is toxic for humans.[23] For this study, an electric field was applied over Pt/TiO_2 catalyst to promote MCH dehydrogenation at lower temperatures without methane or coke by-production. This report is the first of low-temperature and selective catalytic dehydrogenation of MCH over Pt/TiO_2 catalyst in an electric field.

Experimental

Catalyst preparation

For catalyst preparation, platinum was supported on TiO_2 (JRC-TIO-16) and CeO_2 (JRC-CEO-1) using a wet-impregnation method. After catalyst supports were drenched in 25 mL of water for 120 min, Pt precursor, *i.e.* $Pt(NH_3)_4(NO_3)_2$ (Sigma-Aldrich Corp.) was added with 15 mL of diluted water and was dissolved for 120 min in an evaporator. An adequate amount of platinum precursor was introduced to make 3 wt%Pt/TiO_2 and 3 wt%Pt/CeO_2. The obtained solution was dried and calcined at 773 K for 120 min. The resultant catalyst powder was pressed and sieved to 355–500 μm. Prepared catalyst was used for the reaction in the electric field without any pre-treatment.

Catalytic activity tests

A fixed-bed flow type reactor was packed with 200 mg of Pt-supported catalysts to conduct MCH dehydrogenation. An electric field was applied using two stainless steel electrodes set on upper side and bottom side of the catalyst bed. Catalytic dehydrogenation in the electric field was performed by application of 3.0 mA of constant current between two electrodes. The reaction temperature was set between 423 to 773 K with and without the electric field. A thermocouple was placed on the catalyst bed for monitoring the real temperature of the catalyst because Joule heat is expected to increase the catalyst temperature during dehydrogenation in the electric field. T_{tc} stands for the real catalyst temperature measured by the thermocouple. The reaction gas consisted of C_7H_{14} : Ar = 6.4 : 30 (total gas flow rate: 36.4 mL min^{-1}) at ambient pressure of 0.1 MPa. Reactions were conducted in a kinetic region, *i.e.* diffusion is not a rate-determining factor. The gaseous products of the reaction were analyzed using GC-TCD (GC-8A; Shimadzu Corp.) and GC-FID (GC-8A; Shimadzu Corp.). The hydrogen yield was defined using the MCH feed rate (μmol min^{-1}) and H_2 formation rate (μmol min^{-1}).

$$\text{Hydrogen yield (\%)} = r_{H_2}/(C_7H_{14}\text{ feed rate} \times 3) \times 100 \quad (3)$$

The apparent activation energy was estimated over Pt/TiO_2 from Arrhenius plots during MCH dehydrogenation with and without the electric field. Reaction rates were estimated in kinetic control. The reaction rates were calculated from the H_2 formation rate in the same manner as that used for activity tests.

Deposited coke amounts were evaluated using temperature programmed oxidation (TPO) measurements estimating CO or CO_2 formation caused by the oxidation of coke. The temperature was increased from 298 K to 1173 K at 10 K min^{-1} in the gas composition of O_2 : He = 10 : 90 (mL min^{-1}). The product components and coke formation amount indicated a credible mass balance (almost 100%).

Partial pressure dependency and isotope effects

Partial pressure dependencies of MCH, toluene, and hydrogen on reaction rates were evaluated over Pt/TiO_2 catalyst to elucidate the role of the electric field. Results were obtained with and without the electric field at the same MCH-conversion-level *i.e.* (a) at 423 K with the electric field and (b) at 498 K without the electric field. For this experiment, the total feed gas flow was set as 56.4 mL min^{-1} at ambient pressure of 0.1 MPa. Then, the gas ratio was modified as C_7H_{14} : Ar = (3.2, 6.4, 9.6, 11.3) : (53.2, 50.0, 46.8, 45.1), C_7H_{14} : C_7H_8 : Ar = 6.4 : (1.0, 2.0, 3.0, 4.0) : (49.0, 48.0, 47.0, 46.0) and C_7H_{14} : H_2 : Ar = 6.4 : (4.0, 7.0, 9.0, 12.0) : (46.0, 43.0, 41.0, 38.0). Reaction rates were determined by the H_2 formation rate measured using GC-TCD (GC-8A; Shimadzu Corp.).

MCH dehydrogenation was conducted by supplying isotopes of MCH and H_2 to investigate isotope effects with and without the electric field. Accordingly, the reaction gas consisted of C_7H_{14} (or C_7D_{14}; denoted as MCH_D) : H_2 (or D_2) : Ar = 6.4 : 4.0 : 46.0. The total gas flow rate was 56.4 mL min^{-1}. Reaction rates were assessed by the formation rates of H_2, HD, and D_2.

DRIFTS measurements during toluene feed over Pt/TiO_2 and Pt/CeO_2

DRIFTS (diffuse reflectance for infrared Fourier transform spectroscopy) measurements were conducted to investigate toluene adsorption over Pt/TiO_2 and Pt/CeO_2 catalysts using a Fourier transform infrared spectrometer (FT/IR-6100; Jasco Corp.). Teflon-made DRIFTS cells were packed with sieved catalyst, on which two stainless steel electrodes were set to apply the electric field. Detailed information related to the apparatus of DRIFTS measurement is presented elsewhere.[24] Although the electric field was stabilized over Pt/TiO_2 in a fixed-bed flow-type reactor, electrical discharge has occurred all the time over packed Pt/TiO_2 in the DRIFTS cell. Therefore, the experiment with the electric field was performed only over Pt/CeO_2 for safety reasons. Toluene gas was introduced into the measurement chamber for 30 min. Subsequently, in the case of Pt/CeO_2, the feed gas was switched to argon. Then an electric field was applied for 30 min. Subsequently, purge treatment was conducted to extract toluene gas from the chamber atmosphere. The DRIFTS spectra were obtained after each process.

Characterization of catalysts

The metallic surface area of Pt metal was evaluated using CO pulse measurements (Autosorb iQ; Quantachrome Instruments). For vaporizing adsorbed water on the catalyst, pre-treatment was conducted at 673 K in helium. In addition, STEM images and EDX mapping results were obtained from scanning transmission electron microscopy (STEM; HF-2210; Hitachi Ltd.) to confirm the state of Pt over catalytic supports. The specific surface area of catalysts was examined using nitrogen adsorption with the BET method (Gemini VII; Micromeritics Instrument Corp.). For this experiment, pre-treatment

was conducted at 473 K in nitrogen atmosphere for 120 min. Additionally, the electric state of Pt was investigated using XPS measurements (VersaProbe2; ULVAC-PHI, Inc.) without an exposure to air. Orbital $4f_{7/2}$ and $4f_{5/2}$ of Pt were measured. For this experiment, X-ray source was Al Kα. The binding energies were referenced to the C 1s peak at 284.8 eV.

Results and discussion

Promotion effects of electric fields on catalytic activity during MCH dehydrogenation

After various screening tests, we performed MCH dehydrogenation over Pt/TiO_2 catalyst as an optimal catalyst at several temperatures from 423 K to 773 K with and without an electric field (3 mA of constant current). The resultant catalytic activities are presented in Table 1. Although the applied electric field produced little Joule heat, the increase of the catalyst bed temperature (thermocouple temperature, T_{tc}) was no more than 10 K during the reaction. Additionally, the electric field application drastically improved the catalytic activity. The electric field effect was more remarkable at lower temperatures. Especially at 423 K, the catalytic activity was 17.9%, even in a kinetic condition. That activity exceeded the equilibrium limitation (5%) at this temperature.

The values of apparent activation energy were evaluated with and without the electric field to elucidate the promoted catalytic performance of Pt/TiO_2 catalyst by the electric field. Fig. 1 shows Arrhenius plots over Pt/TiO_2 catalyst during MCH dehydrogenation with (filled plots) and without (blank plots) the electric field. According to these results, the respective values of apparent activation energy were 26.9 and 60.7 kJ mol^{-1} with and without the electric field. Such experimental data indicate that the applied electric field facilitated the MCH dehydrogenation, and changed the reaction mechanism.

Kinetic analysis and isotope effect during MCH dehydrogenation in the electric field

To investigate the role of the applied electric field, partial pressure dependencies were evaluated. Fig. 2 presents results of

Table 1 Catalytic activity during MCH dehydrogenation with/without the electric field[a]

Reaction	With EF		Without EF	
Temperature/K	T_{tc}/K	H_2 yield/%	T_{tc}/K	H_2 yield/%
423	432	17.9	423	1.2
473	475	31.7	473	10.9
498	—	—	498	19.0
523	523	58.2	523	32.6
573	573	78.1	573	63.9
623	623	94.4	623	76.1
673	673	99.6	673	88.3
723	723	100.0	723	94.5
773	773	99.9	773	98.8

[a] T_{tc}: catalyst-bed temperature measured with a thermocouple.

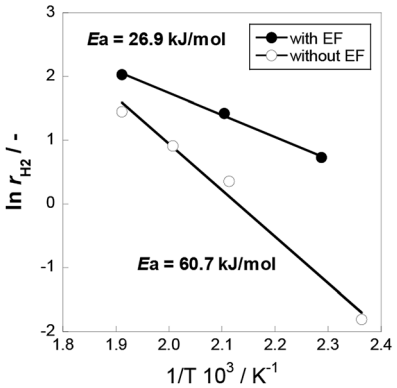

Fig. 1 Arrhenius plots of Pt/TiO_2 with and without the electric field (EF).

partial pressure dependencies of MCH, toluene, and hydrogen. Generally speaking, the catalytic MCH dehydrogenation is a reversible endothermic reaction. The MCH dehydrogenation reaction rate is assumed as the following equation using MCH, toluene, and hydrogen partial pressures.

$$r_{\text{dehydrogenation}} = k[\text{MCH}]^a[\text{Toluene}]^b[\text{H}_2]^c \quad (4)$$

The dehydrogenation rate was correlated positively with the MCH partial pressure similarly in both cases: a was 0.49 with the electric field and 0.47 without the electric field. As results over Pt/TiO_2 catalyst, the toluene partial pressure was unrelated to the dehydrogenation rate; b was zero with and without the electric field. This tendency found for the toluene partial pressure, which differs from the well-known Pt catalyst supported on alumina, has been reported for Pt/TiO_2 catalyst.[25] Accordingly, Pt catalyst supported on TiO_2 is more tolerant of inhibition by toluene adsorption during MCH dehydrogenation. Regarding results of hydrogen partial pressures found with and without the electric field, the MCH dehydrogenation rate was

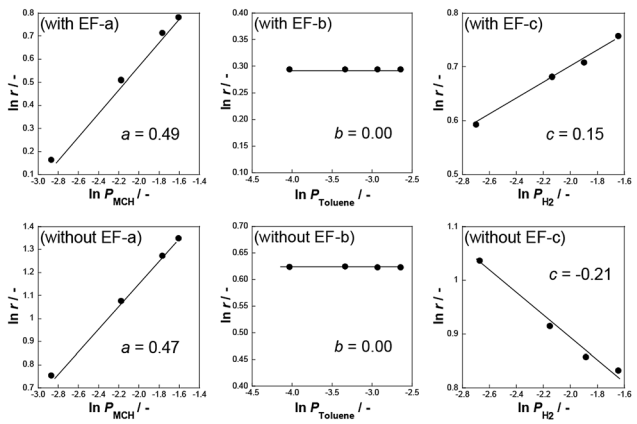

Fig. 2 Partial pressure dependences of (a) methylcyclohexane, (b) toluene, and (c) hydrogen over Pt/TiO_2 for MCH dehydrogenation. Reaction temperature 423 K (with EF), 498 K (without EF), and input current 3 mA.

Table 2 Isotope effect during MCH dehydrogenation over Pt/TiO_2[a]

Condition		T_{tc}/K	H_2 production rate/μmol min^{-1}	H_2 yield/%	k_D/k_H/—
With EF (423 K)	MCH_H/H_2	437	109	13.8	—
	MCH_H/D_2	435	134	17.1	1.24
	MCH_D/H_2	434	135	17.1	1.24
	MCH_D/D_2	433	160	20.3	1.47
Without EF (498 K)	MCH_H/H_2	496	169	21.5	—
	MCH_H/D_2	495	182	23.2	1.08
	MCH_D/H_2	497	111	14.2	0.66
	MCH_D/D_2	496	117	14.9	0.69

[a] T_{tc}: catalyst-bed temperature measured with a thermocouple.

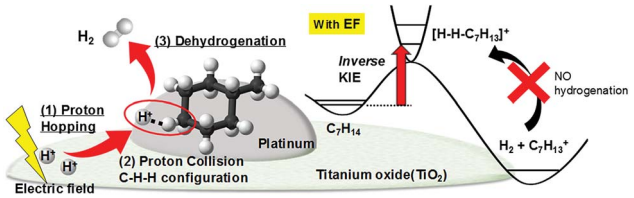

Fig. 3 Mechanism scheme of MCH dehydrogenation over Pt/TiO_2 in the electric field.

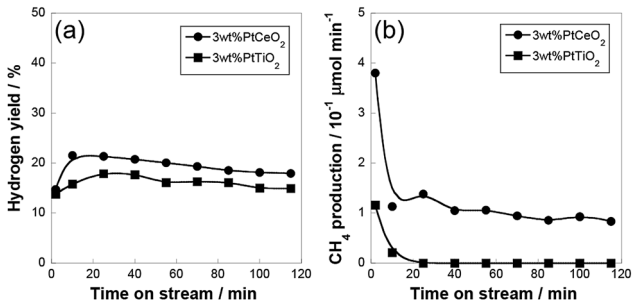

Fig. 4 Results of catalytic activity tests in the electric field over Pt/TiO_2 and Pt/CeO_2 at 423 K: (a) hydrogen yield and (b) CH_4 by-production rate.

negatively correlated by hydrogen without the electric field, c was −0.21. One can infer that hydrogen promoted reverse toluene hydrogenation without the electric field. However, the hydrogen partial pressure was positively correlated with the MCH dehydrogenation rate in the electric field, c, was 0.15, which differs from common results. In earlier studies, such positive values of hydrogen partial pressure dependence are apparent if proton (H^+) hopping occurs on the catalyst surface.[26–28] In the case of methane steam reforming in the electric field, protons hopped on Pd/CeO_2 catalyst surface and facilitated methane activation by proton collision with methane.[24,26] Therefore, protons can function as a reaction promoter during MCH dehydrogenation in the electric field. In the low temperature and low conversion region, toluene and hydrogen, which were products of dehydrogenation had no negative influence on dehydrogenation rate. Therefore, dehydrogenation might proceed with an irreversible process.

To elucidate the role of proton species, isotope effects were confirmed by supplying isotopic MCH_D and D_2 during MCH dehydrogenation with and without the electric field (Table 2). Here, isotope effects were expressed by the ratio of rate

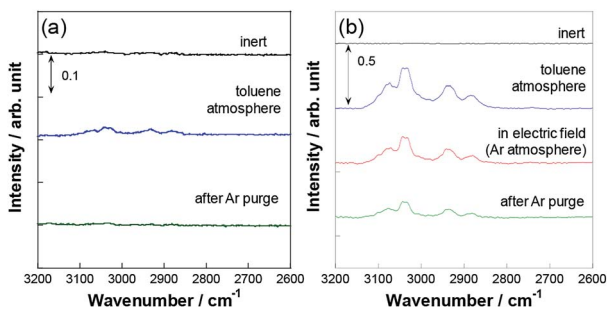

Fig. 5 Spectra of *in situ* DRIFTS measurements of (a) Pt/TiO_2 and (b) Pt/CeO_2 in various conditions at 423 K.

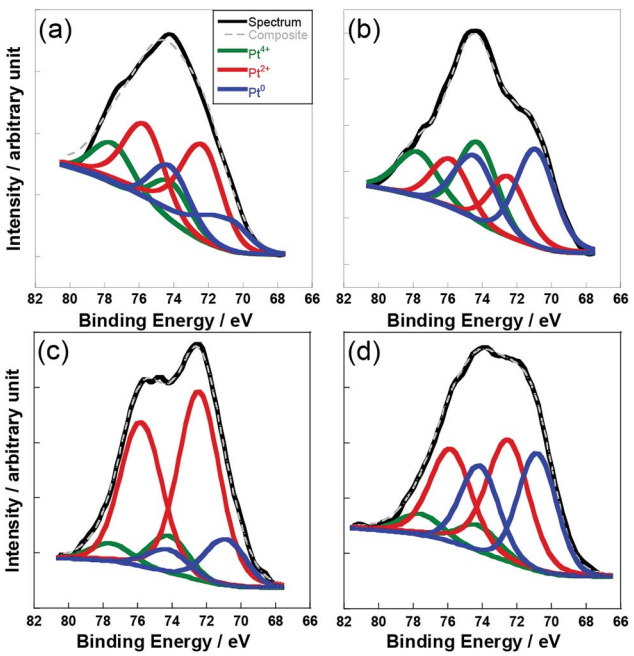

Fig. 6 XPS analysis of the Pt $4f_{7/2}$ and $4f_{5/2}$: (a) Pt/TiO_2 as made, (b) Pt/TiO_2 after EF, (c) Pt/CeO_2 as made, and (d) Pt/CeO_2 after EF.

Table 3 Electronic state of Pt on TiO_2 and CeO_2 from XPS measurement

		Binding energy/eV			Relative peak area/%		
Catalyst	Condition	Pt^0	Pt^{2+}	Pt^{4+}	Pt^0	Pt^{2+}	Pt^{4+}
3 wt% Pt/TiO_2	As made	70.8	72.4	74.2	22.9	52.2	24.9
3 wt% Pt/TiO_2	After reaction with EF (423 K)	70.9	72.5	74.3	43.5	27.1	29.5
3 wt% Pt/CeO_2	As made	70.9	72.4	74.2	16.5	74.8	8.8
3 wt% Pt/CeO_2	After reaction with EF (423 K)	70.8	72.5	74.3	39.8	50.0	10.3

constants (k) with/without isotope, *i.e.* k_D/k_H ratio. Generally, k_D/k_H is a value lower than 1 because chemical bonding of heavier isotopes is more stable (lower zero-point energy: ZPE).[29] Without the electric field, the results follow these general trends when isotope MCH_D was introduced, k_D/k_H was 0.66 with MCH_D/H_2 and k_D/k_H was 0.69 with MCH_D/D_2. Accordingly, the kinetic isotope effect (KIE) was confirmed without the electric field. Nevertheless, with the electric field, k_D/k_H increased as a larger proportion of deuterium was introduced into the reactor, as shown in Table 2. This inverse KIE has been observed when C–H–H configuration was formed through proton collision,[24] explained by the ZPE discrepancy on isotopes.[24,30–34] During MCH dehydrogenation in the electric field, inverse KIE are observed by the collision of accelerated proton with H (or D)-atoms of MCH to form [H (or D)–H (or D)–C_7H_{13}]$^+$ over Pt/TiO_2 catalyst, to advance the reaction of MCH dehydrogenation further. After dehydrogenation, the resultant state of $C_7H_{13}^+$ + H_2 has much lower energy level than the three-atom transition and the initial physisorption state (Fig. 3). In this case, reverse hydrogenation has larger activation energy, making it difficult to proceed.[24,31,32,34] Thereby, results suggest that the applied electric field promoted proton hopping and MCH dehydrogenation to show higher catalytic activity beyond the equilibrium limitation (Fig. 3).

Methane by-production suppression and the electric state of platinum on Pt/TiO_2 catalyst

Methane by-production rate and coke deposition over Pt/TiO_2 catalyst were investigated during MCH dehydrogenation at 423 K in the electric field. Only slight to no coke deposition occurred in this catalyst system (ESI Table S1†). Also, the structure of catalyst was not changed even after the reaction in the electric field (ESI Table S2†). Fig. 4 presents results of the catalytic activity and methane by-production rate during 120 min of dehydrogenation. For better comparison, results over Pt/CeO_2 catalyst are also presented in Fig. 4. Results show that Pt/TiO_2 had no methane by-production after 10–25 min of dehydrogenation as the applied electric field being stabilized. According to the partial pressure dependency of toluene, Pt/TiO_2 catalyst showed high tolerance against inhibition by toluene adsorption during MCH dehydrogenation both with and without the electric field. Methane by-production reportedly occurs with hydrodemethylation of produced toluene during MCH dehydrogenation. Consequently, the toluene behavior over Pt/TiO_2 is regarded as related to the methane by-production rate during dehydrogenation.

DRIFTS measurements were conducted over Pt/TiO_2 and Pt/CeO_2 catalysts supplying toluene on the catalyst surface, as shown in Fig. 5. In the case of Pt/TiO_2, the electric field cannot be stable and applicable in the DRIFTS system because of the cell structure. Therefore, *in situ* DRIFTS with the electric field was conducted over Pt/CeO_2 instead of Pt/TiO_2. Regarding the Pt/CeO_2 catalyst, toluene adsorption was observed both with and without the electric field (C–H stretching around 3000 cm^{-1}).[35,36] However, the IR peaks for toluene are barely visible over Pt/TiO_2 catalyst, even under a toluene atmosphere. Furthermore, the peaks disappeared completely after purge treatment. These results demonstrate that Pt/TiO_2 catalyst can suppress toluene adsorption and methane by-production during MCH dehydrogenation.

Fig. 6 and Table 3 present results of XPS measurements for Pt over Pt/TiO_2 and Pt/CeO_2. The XPS peaks for $4f_{7/2}$ and $4f_{5/2}$ orbitals are divisible into three states: Pt^0, Pt^{2+}, and Pt^{4+}.[37] Here, Pt^{4+} was assumed as embedded Pt with strong metal and support interaction (SMSI). As SMSI is known to occur readily between Pt and TiO_2 (ref. 25) because Pt is highly dispersed and not aggregated (shown in ESI Fig. S2†), it might be the reason why Pt/TiO_2 showed lower surface area than Pt/CeO_2 did (ESI Table S2†). Larger amounts of Pt might be embedded inside the TiO_2 support. Pt reducibility was estimated and compared over Pt/TiO_2 and Pt/CeO_2 from the ratio of $(Pt^0 + Pt^{2+})/Pt^{4+}$. Pt on TiO_2 showed more peak area for Pt^{4+} even after the reaction in the electric field, so the reducibility of Pt^{4+} in/on TiO_2 seems low due to the SMSI. On the other hand, comparing Pt^{2+} and Pt^0, Pt on Pt/TiO_2 is more metallic after the reaction in the electric field. It has been described in earlier reports that supported Pt is more easily reduced in the electric field,[38] and TiO_2 can donate electrons to Pt.[25] The interaction between Pt and π-coordination of toluene can be weakened over reductive Pt.[25] Consequently, reductive Pt over Pt/TiO_2 catalyst is important for high tolerance against toluene inhibition and methane by-production.

Conclusions

Dehydrogenation of methylcyclohexane (MCH) was conducted over Pt/TiO_2 catalyst by applying an electric field. The electric field promoted the reaction to achieve 17.9% hydrogen yield, even at 423 K and a kinetic condition, under which the catalytic activity exceeded the equilibrium limitation (5%). Despite the reversibility of dehydrogenation, the reaction rate was positively correlated with the partial pressure of hydrogen with the electric

field application. Additionally, an inverse kinetic isotope effect (KIE) was observed with isotope MCH_D (C_7D_{14}) and D_2 in the electric field. These results indicate that hydrogen-derived species, *i.e.* protons, promoted the abstraction of H-atoms from MCH for dehydrogenation. Furthermore, Pt/TiO_2 catalyst, different from other catalysts, showed neither methane nor coke by-production during MCH dehydrogenation in the electric field at 423 K. DRIFTS measurements revealed that toluene was only slightly adsorbed over Pt/TiO_2 catalyst. XPS measurements demonstrated that Pt on TiO_2 was more metallic after applying the electric field. Actually, TiO_2 is known to be capable of donating electrons to the empty orbital of Pt. Therefore, we inferred that more metallic Pt on TiO_2 support weakened interaction between Pt and π-coordination of toluene. In conclusion, results show that Pt/TiO_2 catalyst promotes MCH dehydrogenation selectively at low temperatures by virtue of proton hopping in the electric field.

Conflicts of interest

There are no conflicts to declare.

Acknowledgements

This study was supported by JST-CREST JPMJCR1423 and JSPS Grants-in-Aid for Scientific Research – KAKENHI.

References

1 M. Balat, *Int. J. Hydrogen Energy*, 2008, **33**, 4013–4029.
2 T. Sinigaglia, F. Lewiski, M. Eduardo, S. Martins and J. C. M. Siluk, *Int. J. Hydrogen Energy*, 2017, **42**, 24597–24611.
3 S. Sharma and S. K. Ghoshal, *Renewable Sustainable Energy Rev.*, 2015, **43**, 1151–1158.
4 A. Klerke, C. H. Christensen, J. K. Norskov and T. Vegge, *J. Mater. Chem.*, 2008, **18**, 2304–2310.
5 R. Lan, J. T. S. Irvine and S. Tao, *Int. J. Hydrogen Energy*, 2012, **37**, 1482–1494.
6 F. Alhumaidan, D. Cresswell and A. Garforth, *Energy Fuels*, 2011, **25**, 4217–4234.
7 E. Gianotti, M. Taillades-Jacquin, J. Roziere and D. J. Jones, *ACS Catal.*, 2018, **8**, 4660–4680.
8 Y. Okada, E. Sasaki, E. Watanabe, S. Hyodo and H. Nishijima, *Int. J. Hydrogen Energy*, 2006, **31**, 1348–1356.
9 R. B. Biniwale, S. Rayalu, S. Devotta and M. Ichikawa, *Int. J. Hydrogen Energy*, 2008, **33**, 360–365.
10 A. Shukla, J. Pande and R. B. Biniwale, *Int. J. Hydrogen Energy*, 2012, **37**, 3350–3357.
11 N. Boufaden, R. Akkari, B. Pawelec, J. L. G. Fierro, M. S. Zina and A. Ghorbel, *J. Mol. Catal. A: Chem.*, 2016, **420**, 96–106.
12 L. W. Jossens and E. E. Petersen, *J. Catal.*, 1982, **73**, 377–386.
13 B. Liu, Z. Wang, Q. Zhu, X. Li and J. Wang, *Fuel*, 2017, **200**, 387–394.
14 G. Maria, A. Marin, C. Wyss, S. Muller and E. Newson, *Chem. Eng. Sci.*, 1996, **51**, 2891–2896.
15 W. Wang, L. Miao, K. Wu, G. Chen, Y. Huang and Y. Yang, *Int. J. Hydrogen Energy*, 2019, **44**, 2918–2925.
16 D. K. Cromwell, P. T. Vasudevan, B. Pawelec and J. L. G. Fierro, *Catal. Today*, 2016, **259**, 119–129.
17 N. Boufaden, R. Akkari, B. Pawelec, J. L. G. Fierro, M. Said Zina and A. Ghorbel, *Appl. Catal., A*, 2015, **502**, 329–339.
18 N. Boufaden, B. Pawelec, J. L. G. Fierro, R. Guil López, R. Akkari and M. Said Zina, *Mater. Chem. Phys.*, 2018, **209**, 188–199.
19 A. Nakano, S. Manabe, T. Higo, H. Seki, S. Nagatake, T. Yabe, S. Ogo, T. Nagatsuka, Y. Sugiura, H. Iki and Y. Sekine, *Appl. Catal., A*, 2017, **543**, 75–81.
20 Y. Sugiura, T. Nagatsuka, K. Kubo, Y. Hirano, A. Nakamura, K. Miyazawa, Y. Iizuka, S. Furuta, H. Iki, T. Higo and Y. Sekine, *Chem. Lett.*, 2017, **46**(11), 1601–1604.
21 S. Manabe, T. Yabe, A. Nakano, S. Nagatake, T. Higo, S. Ogo, H. Nakai and Y. Sekine, *Chem. Phys. Lett.*, 2018, **711**, 73–76.
22 F. Alhumaidan, D. Tsakiris, D. Cresswell and A. Garforth, *Int. J. Hydrogen Energy*, 2013, **32**, 14010–14026.
23 W. F. Greenlee, J. D. Sun and J. S. Bus, *Toxicol. Appl. Pharmacol.*, 1981, **59**, 187–195.
24 S. Okada, R. Manabe, R. Inagaki, S. Ogo and Y. Sekine, *Catal. Today*, 2018, **307**, 272–276.
25 S. Nagatake, T. Higo, S. Ogo, Y. Sugiura, R. Watanabe, C. Fukuhara and Y. Sekine, *Catal. Lett.*, 2016, **146**, 54–60.
26 R. Manabe, S. Okada, R. Inagaki, K. Oshima, S. Ogo and Y. Sekine, *Sci. Rep.*, 2016, **6**, 38007.
27 K. Oshima, T. Shinagawa, Y. Nogami, R. Manabe, S. Ogo and Y. Sekine, *Catal. Today*, 2014, **232**, 27–32.
28 R. Inagaki, R. Manabe, Y. Hisai, Y. Kamite, T. Yabe, S. Ogo and Y. Sekine, *Int. J. Hydrogen Energy*, 2018, **43**, 14310–14318.
29 G. A. Olah and R. H. Schlosberg, *J. Am. Chem. Soc.*, 1968, **90**, 2726–2727.
30 G. A. Olah, G. Klopman and R. H. Schlosberg, *J. Am. Chem. Soc.*, 1969, **91**, 3261–3268.
31 G. C. Schatz and A. F. Wagner, *J. Phys. Chem.*, 2018, **88**, 221–232.
32 B. Kerkeni and D. C. Clary, *J. Phys. Chem. A*, 2004, **108**, 8966–8972.
33 K. B. Wiberg, *Chem. Rev.*, 1955, **55**, 713–743.
34 M. J. Kurylo, G. A. Hollinden and R. B. Timmons, *J. Chem. Phys.*, 1970, **52**, 1773–1781.
35 M. D. Hernandez, I. Tejedor-Tejedor, J. M. Coronado and M. A. Andreson, *Appl. Catal., B*, 2011, **101**, 283–293.
36 D. Murzin, T. Salmi, S. Smeds, M. Laatikainen, M. Mustonen and E. Paatero, *React. Kinet. Catal. Lett.*, 1997, **61**, 227–236.
37 P. Bera, K. R. Priolkar, A. Gayen, P. R. Sarode, M. S. Hegde, S. Emura, R. Kumashiro, V. Jayaram and G. N. Subbanna, *Chem. Mater.*, 2003, **15**, 2049–2060.
38 S. Sakurai, S. Ogo and Y. Sekine, *J. Jpn. Pet. Inst.*, 2016, **59**(5), 174–183.

